Communication

# An NMR Experiment for Simultaneous TROSY-Based Detection of Amide and Methyl Groups in Large Proteins

Chenyun Guo, Daoning Zhang, and Vitali Tugarinov

*J. Am. Chem. Soc.*, **2008**, 130 (33), 10872-10873 • DOI: 10.1021/ja8036178 • Publication Date (Web): 24 July 2008



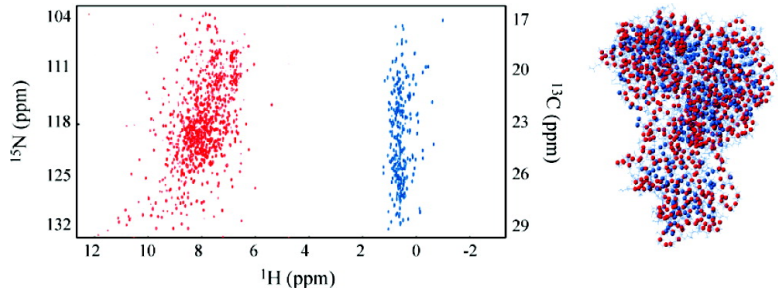


## More About This Article

Additional resources and features associated with this article are available within the HTML version:

- Supporting Information
- Access to high resolution figures
- Links to articles and content related to this article
- Copyright permission to reproduce figures and/or text from this article

View the Full Text HTML

J|A|C|S
COMMUNICATIONS

Published on Web 07/24/2008

# An NMR Experiment for Simultaneous TROSY-Based Detection of Amide and Methyl Groups in Large Proteins

Chenyun Guo, Daoning Zhang, and Vitali Tugarinov*

*Department of Chemistry and Biochemistry, University of Maryland, College Park, Maryland 20742*

Received May 15, 2008; E-mail: vitali@umd.edu

Transverse relaxation optimized spectroscopy[1] (TROSY) techniques in tandem with high levels of deuteration facilitate NMR studies of increasingly large protein molecules and macromolecular assemblies.[2] Since the original development of $^{15}N-^{1}H$ TROSY,[1] the principles of TROSY have been extended to several other spin systems encountered in proteins.[3–5] Methyl-TROSY[5] coupled with selective $^{13}CH_3$ labeling of Ile, Leu, and Val side chains in otherwise deuterated proteins has proven especially valuable for a number of NMR studies of structure and dynamics of very large protein systems.[6–9]

The principle of TROSY is based upon isolation of slowly relaxing components of NMR signals.[1] In terms of experimental design that means that the slowly relaxing coherences evolving during the indirect detection period ($t_1$) of a 2D NMR experiment are to be selectively transferred to the slowly relaxing components evolving during signal acquisition ($t_2$) in a manner that precludes an intermix between the "slow" and "fast" parts of the signal. In the case of Methyl-TROSY, this is achieved by the simple HMQC[10,11] experiment.[5] However, preservation of both orthogonal components of the coherences evolving during $t_1$ periods (preservation of equivalent pathways, PEP), accompanied by an $\sim\sqrt{2}$ increase in sensitivity,[12,13] intrinsic to all implementations of $^{15}N-^{1}H$ TROSY, is not easily achieved for $^{13}CH_3$ methyls attached to large macromolecules. Here, we describe a 2D NMR experiment for time-shared TROSY-based detection of amide ($^{1}H-^{15}N$) and methyl ($^{13}CH_3$) groups in large proteins that utilizes gradient-enhanced preservation of equivalent pathways for both types of spin systems simultaneously.

Formally, the gradient-selected PEP-HMQC pulse scheme shown in Figure 1 satisfies the main requirements of the TROSY magnetization transfer. Both orthogonal parts of the slowly relaxing component (central line of the multiple-quantum methyl triplet) present during the $t_1$ period are transferred to the slowly relaxing proton coherences for acquisition ($t_2$), so that between points *a* and *d* in the scheme of Figure 1,

$$\sum_{i,j,k=1}^{3}\left\{C_y H_x^i - 4C_y H_x^i H_z^j H_z^k\right\}\cos(\omega_C t_1) \rightarrow \sum_{i,j,k=1}^{3}\left\{-\frac{1}{2}H_y^i + 2H_y^i H_z^j H_z^k\right\}\cos(\omega_C t_1) \quad (1)$$

and

$$\sum_{i,j,k=1}^{3}\left\{C_x H_x^i - 4C_x H_x^i H_z^j H_z^k\right\}\sin(\omega_C t_1) \rightarrow \sum_{i,j,k=1}^{3}\left\{\frac{1}{2}H_x^i - 2H_x^i H_z^j H_z^k\right\}\sin(\omega_C t_1) \quad (2)$$

where $C_r^i$ and $H_r^i$ are product operators for carbon and proton nuclei, respectively, $r = x,y,z$, and the sums run over all the methyl protons

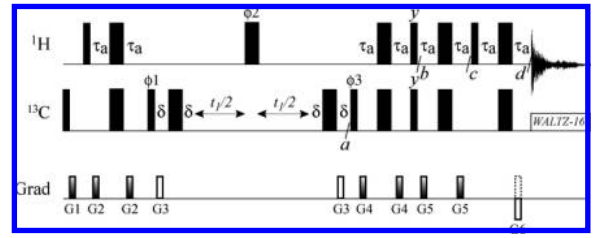


***Figure 1.*** Pulse scheme for gradient-enhanced preservation of equivalent pathways in $^{13}CH_3$ methyls of large proteins. All narrow(wide) rectangular pulses are applied with flip angles of 90(180)° along the *x*-axis unless indicated otherwise. All $^{1}H$ and $^{13}C$ pulses are applied with the highest possible power; $^{13}C$ WALTZ-16 decoupling is achieved using a 2-kHz field. Delays are: $\tau_a = 2.0$ ms; $\delta = 500\ \mu s$. The durations and strengths of pulsed-field gradients in units of (ms;G/cm) are as follows: G1 = (1;15), G2 = (0.3;10), G3 = (0.4;20), G4 = (0.25;15), G5 = (0.3;12), G6 = (0.4;−10). Phase cycle: $\phi1 = x,-x$; $\phi2 = 2(x),2(-x)$; $\phi3 = x$; rec. $= x,-x$. Quadrature detection in $t_1$ is achieved via a gradient enhanced sensitivity scheme: for each $t_1$ value a pair of spectra are recorded with $\phi3 = x$;G6 and $\phi3 = -x$;−G6 and manipulated postacquisition.[12–14] The phase $\phi1$ is inverted for each $t_1$ point.

($i \neq j \neq k$), relaxation and the effect of gradients are neglected, and we concentrate only on the slowly relaxing parts of the signal. The phase-modulated signal represented by the sum and difference of eqs 1 and 2 can be acquired and processed using the standard gradient enhanced sensitivity scheme.[12–14] The two orthogonal pathways have very different relaxation properties and have to be "balanced" by the use of gradient coherence selection. Of note, since the slow- and fast-relaxing components of the signal evolve during $t_2$ in the opposite senses, the fast-relaxing part can be selected for, if desired, simply by inversion of the sign of the gradient G6 (Figure 1).

However, this experiment does not lead to sensitivity gains when compared to methyl-HMQC due to significant relaxation losses occurring during the time period between points *b* and *c* (Figure 1) when a part of the "slow" methyl coherences is temporarily transferred to "fast" components in one of the two orthogonal pathways. This represents a serious limitation of the scheme in Figure 1. In fact, the average signal-to-noise ratio achieved in the spectra recorded with the scheme of Figure 1 was only ~75 ± 25% of that obtained in HMQC experiment recorded on both {U-[$^{15}N$,$^{2}H$]; Ile-[$^{13}CH_3$]; Leu,Val-[$^{13}CH_3/^{12}CD_3$]}-labeled 8.5-kDa Ubiquitin (UBI, 27 °C) and 82-kDa Malate Synthase G (MSG, 37 °C). In smaller proteins, a portion of these losses arises from gradient selection of the "slow" part of the signal that contributes only ~75%(85%) of the total methyl signal in UBI at 27 °C(5 °C).

The PEP-HMQC scheme of Figure 1 can be put to good use when integrated into a more complicated pulse scheme for simultaneous detection of $^{13}CH_3$ and $^{1}H-^{15}N$ regions in NMR spectra of large proteins. Such a pulse scheme is presented in Figure 2a, where TROSY-type magnetization transfer in $^{13}CH_3$ groups (see


10.1021/ja8036178 CCC: $40.75 

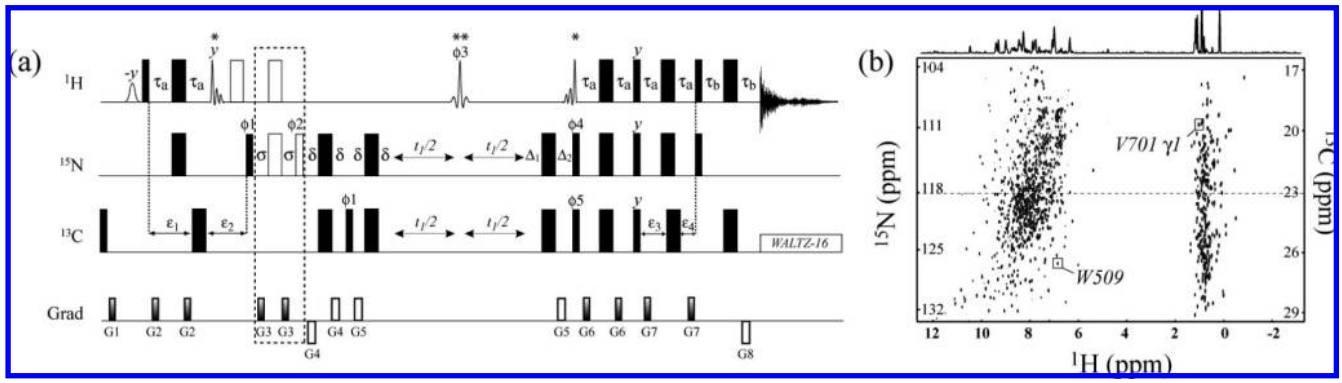


***Figure 2.*** (a) Simultaneous 2D $^1H-^{15}N/^{13}CH_3$ TROSY pulse scheme (see Figure 1 for definitions). The $^1H$, $^{15}N$, and $^{13}C$ carrier frequencies are positioned at 4.7, 119, and 23 ppm, respectively. The first water-selective $^1H$ pulse has an E-BURP-1[16] shape and duration of 7 ms. Two $^1H$ pulses marked with asterisks are 1.25 ms time-reversed SNEEZE[17] (phase $y$) and SNEEZE[17] shapes, respectively, (600 MHz) with the center of excitation shifted to 8 ppm via phase modulation of RF field for excitation of amide protons and the water signal. The pulse marked with double asterisks ($\phi 3$) is a 1.25 ms RE-BURP[16] pulse centered at −1.1 ppm via phase modulation of RF field for selective refocusing of methyl protons. Delays are as follows: $\tau_a = 2.3$ ms; $\tau_b = 2$ ms; $\sigma = 1.33$ ms; $\delta = 0.5$ ms; $\epsilon_1 = 3.1$ ms; $\epsilon_2 = 2.5$ ms; $\epsilon_3 = 2.6$ ms; $\epsilon_4 = 2.0$ ms. Delays $\Delta_i$ are carefully adjusted to avoid evolution of methyl $^1H$ chemical shifts before and during $t_1$ period: $\Delta_1 = 3\delta + pw_N$; $\Delta_2 = 3\delta + pw_N + P_{\phi 3}$, where $pw_N$ is the length of nitrogen pulse, and $P_{\phi 3}$ is the length of the RE-BURP pulse. Durations and strengths of pulsed-field gradients in units of (ms;G/cm) are as follows: G1 = (1;15); G2 = (0.3;5); G4 = (0.35;24); G5 = (0.35;16); G6 = (0.25;15); G7 = (0.3;20); G8 = (0.35;−8). Phase cycle: $\phi 1 = 2(x),2(-x)$; $\phi 3 = y,-y$; $\phi 4 = \phi 5 = x$; rec. $= 2(x),2(-x)$. Quadrature detection in $t_1$ is achieved via a gradient enhanced sensitivity scheme: for each $t_1$ value a pair of spectra are recorded with $\phi 4$, $\phi 5 = x$;G8 and $\phi 4$, $\phi 5 = -x$;−G8 and manipulated postacquisition.[12–14] The phase $\phi 1$ is inverted for each $t_1$ point. For active suppression of the anti-$^1H-^{15}N$ TROSY component (not employed for MSG) the element enclosed in the dashed box should be included together with the adjacent open $^1H$ $\pi$ pulse.[15] Then, G3 = (0.3;12); $\phi 2 = 2(45°),2(225°)$, and $\phi 4$ should be incremented by 45° in order to ensure the same phase for methyl and amide signals in $t_1$. (b) Simultaneous $^1H-^{15}N/^{13}CH_3$ correlation map recorded using the pulse sequence shown in (a) on the 0.5 mM sample of {U-[$^{15}N$,$^2H$]; Ile-[$^{13}CH_3$]; Leu,Val-[$^{13}CH_3/^{12}CD_3$]}-labeled MSG (37 °C, 600 MHz, 90% $H_2O$/10% $D_2O$, glyoxylate concentration = 250 $\mu$M). Spectral width is adjusted so that all the peaks of isoleucine methyls are aliased. Labeling of $F_1$ axis with $^{15}N/^{13}C$ in units of ppm is solely for illustration purposes.

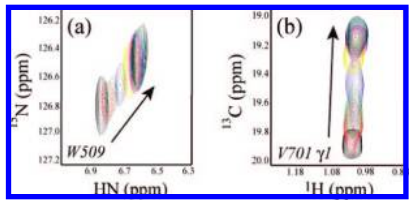


***Figure 3.*** Typical examples of chemical shift changes occurring upon addition of glyoxylate to MSG for (a) the amide peak of W509 and (b) V701 $\gamma 1$ methyl. The spectra were recorded as described in Figure 2.

above) is synchronized with the TROSY transfer in $^1H-^{15}N$ amides implemented as described by Yang and Kay.[15]

Separation between chemical shifts of amide and methyl proton signals in $t_1$ preserves "slow" multiple-quantum coherences of $^{13}CH_3$ without disturbing the slowly relaxing component of $^1H-^{15}N$ amides through the use of selective proton pulses (Figure 2a). Gradient strengths are adjusted for simultaneous selection of slowly relaxing components of $^1H-^{15}N$ and $^{13}CH_3$ signals. Although the proposed experiment proves on average 24%(35%) less sensitive than individual $^1H-^{15}N$ TROSY[15] (HMQC[5,10]) experiments recorded on MSG ($H_2O$, 37 °C), it translates to approximately the same sensitivity per unit of acquisition time. Optimal sensitivity in methyl-TROSY spectra of large proteins is, however, achieved when the spectra are recorded in $D_2O$, an advantage that has to be traded for the convenience of observing both $^1H-^{15}N$ and $^{13}CH_3$ correlation maps simultaneously.

The scheme of Figure 2 is well suited for NMR studies of ligand binding to large proteins labeled with $^{15}N$ and selectively labeled with $^{13}CH_3$ at a number of methyl sites. Methyls are more likely to be positioned in the vicinity of protein binding sites than backbone amides[18] that are, nevertheless, more frequently used for NMR-based screening. The experiment of Figure 2 allows one to derive parameters of ligand binding to large proteins from the amide and methyl regions of a single 2D spectrum. Figure 2b shows such a 2D $^1H-^{15}N/^{13}CH_3$ correlation map obtained for the first titration point of a 723-residue MSG with its native substrate glyoxylate. Figures 3a,b show typical examples of ligand-induced changes in chemical shifts of MSG. The methyl shift-derived dissociation constant of the enzyme−substrate complex ($K_d = 543 \pm 27$ $\mu$M from 12 methyl peaks) is in excellent agreement with its amide-derived counterpart ($K_d = 546 \pm 31$ $\mu$M from 14 amide peaks). We expect that the simultaneous $^1H-^{15}N/^{13}C$ detection scheme described here will serve as a useful addition to the array of available TROSY-based techniques that facilitate NMR studies of large proteins.

**Acknowledgment.** This work was supported in part by the University of Maryland Biotechnology Award to V.T.

## References

(1) Pervushin, K.; Riek, R.; Wider, G.; Wüthrich, K. *Proc. Natl. Acad. Sci. U.S.A.* **1997**, *94*, 12366–12371.
(2) Fernandez, C.; Wider, G. *Curr. Opin. Struct. Biol.* **2003**, *13*, 570–580.
(3) Pervushin, K.; Riek, R.; Wider, G.; Wüthrich, K. *J. Am. Chem. Soc.* **1998**, *120*, 6394–6400.
(4) Miclet, E.; Williams, D. C., Jr.; Clore, G. M.; Bryce, D. L.; Boisbouvier, J.; Bax, A. *J. Am. Chem. Soc.* **2004**, *126*, 10560–70.
(5) Tugarinov, V.; Hwang, P. M.; Ollerenshaw, J. E.; Kay, L. E. *J. Am. Chem. Soc.* **2003**, *125*, 10420–10428.
(6) Sprangers, R.; Kay, L. E. *Nature.* **2007**, *445*, 618–22.
(7) Hamel, D. J.; Dahlquist, F. W. *J. Am. Chem. Soc.* **2005**, *127*, 9676–7.
(8) Sprangers, R.; Gribun, A.; Hwang, P. M.; Houry, W. A.; Kay, L. E. *Proc. Natl. Acad. Sci. U.S.A.* **2005**, *102*, 16678–16683.
(9) Velyvis, A.; Yang, Y. R.; Schachman, H. K.; Kay, L. E. *Proc. Natl. Acad. Sci. U.S.A.* **2007**, *104*, 8815–20.
(10) Bax, A.; Griffey, R. H.; Hawkings, B. L. *J. Magn. Reson.* **1983**, *55*, 301–315.
(11) Mueller, L. *J. Am. Chem. Soc.* **1979**, *101*, 4481–4484.
(12) Palmer, A. G.; Cavanagh, J.; Wright, P. E.; Rance, M. *J. Magn. Reson.* **1991**, *93*, 151–170.
(13) Kay, L. E.; Keifer, P.; Saarinen, T. *J. Am. Chem. Soc.* **1992**, *114*, 10663–10665.
(14) Schleucher, J.; Sattler, M.; Griesinger, C. *Angew. Chem., Int. Ed. Engl.* **1993**, *32*, 1489–1491.
(15) Yang, D.; Kay, L. E. *J. Biomol. NMR* **1999**, *13*, 3–10.
(16) Geen, H.; Freeman, R. *J. Magn. Reson.* **1991**, *93*, 93–141.
(17) Nuzillard, J. M.; Freeman, R. *J. Magn. Reson. A* **1994**, *110*, 252–258.
(18) Hajduk, P. J.; Augeri, D. J.; Mack, J.; Mendoza, R.; Yang, J. G.; Betz, S. F.; Fesik, S. W. *J. Am. Chem. Soc.* **2000**, *122*, 7898–7904.

JA8036178